Am. J. Hum. Genet. 66:1744–1756, 2000

A Novel Disorder Caused by Defective Biosynthesis of N-Linked Oligosaccharides Due to Glucosidase I Deficiency

Claudine M. De Praeter,[1] Gerrit J. Gerwig,[6] Ernst Bause,[7] Lieve K. Nuytinck,[4] Johannes F. G. Vliegenthart,[6] Wilhelm Breuer,[7] Johannis P. Kamerling,[6] Marc F. Espeel,[5] Jean-Jacques R. Martin,[8] Anne M. De Paepe,[4] Nora Wen Chun Chan,[9] Georges A. Dacremont,[3] and Rudy N. Van Coster[2,3]

Department of Pediatrics, Divisions of [1]Neonatal Intensive Care, [2]Pediatric Neurology, and [3]Metabolic Diseases, and [4]Center for Medical Genetics, Ghent University Hospital; [5]Department of Histology and Embryology, Ghent University, Ghent; [6]Department of Bio-Organic Chemistry, Bijvoet Center for Biomolecular Research, Utrecht University, Utrecht; [7]Institut für Physiologische Chemie, Universität Bonn, Bonn; [8]Born-Bunge Foundation, Antwerp University, Antwerp; and [9]Department of Chemistry, University of Alberta, Edmonton

Glucosidase I is an important enzyme in N-linked glycoprotein processing, removing specifically distal α-1,2–linked glucose from the $Glc_3Man_9GlcNAc_2$ precursor after its en bloc transfer from dolichyl diphosphate to a nascent polypeptide chain in the endoplasmic reticulum. We have identified a glucosidase I defect in a neonate with severe generalized hypotonia and dysmorphic features. The clinical course was progressive and was characterized by the occurrence of hepatomegaly, hypoventilation, feeding problems, seizures, and fatal outcome at age 74 d. The accumulation of the tetrasaccharide Glc(α1-2)Glc(α1-3)Glc(α1-3)Man in the patient's urine indicated a glycosylation disorder. Enzymological studies on liver tissue and cultured skin fibroblasts revealed a severe glucosidase I deficiency. The residual activity was <3% of that of controls. Glucosidase I activities in cultured skin fibroblasts from both parents were found to be 50% of those of controls. Tissues from the patient subjected to SDS-PAGE followed by immunoblotting revealed strongly decreased amounts of glucosidase I protein in the homogenate of the liver, and a less-severe decrease in cultured skin fibroblasts. Molecular studies showed that the patient was a compound heterozygote for two missense mutations in the glucosidase I gene: (1) one allele harbored a G→C transition at nucleotide (nt) 1587, resulting in the substitution of Arg at position 486 by Thr (R486T), and (2) on the other allele a T→C transition at nt 2085 resulted in the substitution of Phe at position 652 by Leu (F652L). The mother was heterozygous for the G→C transition, whereas the father was heterozygous for the T→C transition. These base changes were not seen in 100 control DNA samples. A causal relationship between the α-glucosidase I deficiency and the disease is postulated.

Introduction

Glycoproteins play important roles in many biological processes. Their N- and/or O-linked carbohydrate chains are involved in polypeptide folding and stabilizing protein conformation and can act as targeting signals or as ligands for cell-surface receptors mediating cell-cell interaction and recognition (Montreuil et al. 1995). The biosynthesis of N-linked glycans is a complex process, comprising transfer of a preformed $Glc_3Man_9GlcNAc_2$ precursor oligosaccharide to the polypeptide and, subsequently, a series of processing reactions catalyzed by glycosidases and glycosyltransferases (Montreuil et al. 1996*a*) (fig. 1).

Inborn errors in the glycan biosynthesis may have dramatic influences on the properties and functioning of the glycoproteins and may lead to severe clinical syndromes. Defects in the biosynthetic pathway may occur either in the assembly reactions of the precursor oligosaccharide or in enzymatic processing. Deficiencies of the enzymes involved represent the main causes of these autosomal recessive diseases (Kornfeld 1998). Only five primary disorders due to defective N-glycosylation of glycoproteins have been identified: (1) mucolipidosis II (I-cell disease) (MIM 252500) and mucolipidosis III (MIM 252600) (pseudo-Hurler polydystrophy) (Reitman et al. 1981); (2) leukocyte adhesion deficiency, type II (MIM 266265) (Etzioni et al. 1992); (3) congenital dyserythropoietic anemia type II (HEMPAS disease) (MIM 224100) (Fukada 1990); (4) paroxysmal nocturnal hemoglobinuria (MIM 311770) (Rosse 1997); and (5) carbohydrate-deficient glycoprotein syndrome (CDGS) (MIM 212065, MIM

Received November 30, 1999; accepted for publication March 14, 2000; electronically published April 28, 2000.

Address for correspondence and reprints: Dr. Rudy N. Van Coster, Pediatric Neurology and Metabolic Diseases, Ghent University Hospital, De Pintelaan, 185, B9000 Ghent, Belgium. E-mail: rudy.vancoster@rug.ac.be

0002-9297/2000/6606-0004$02.00

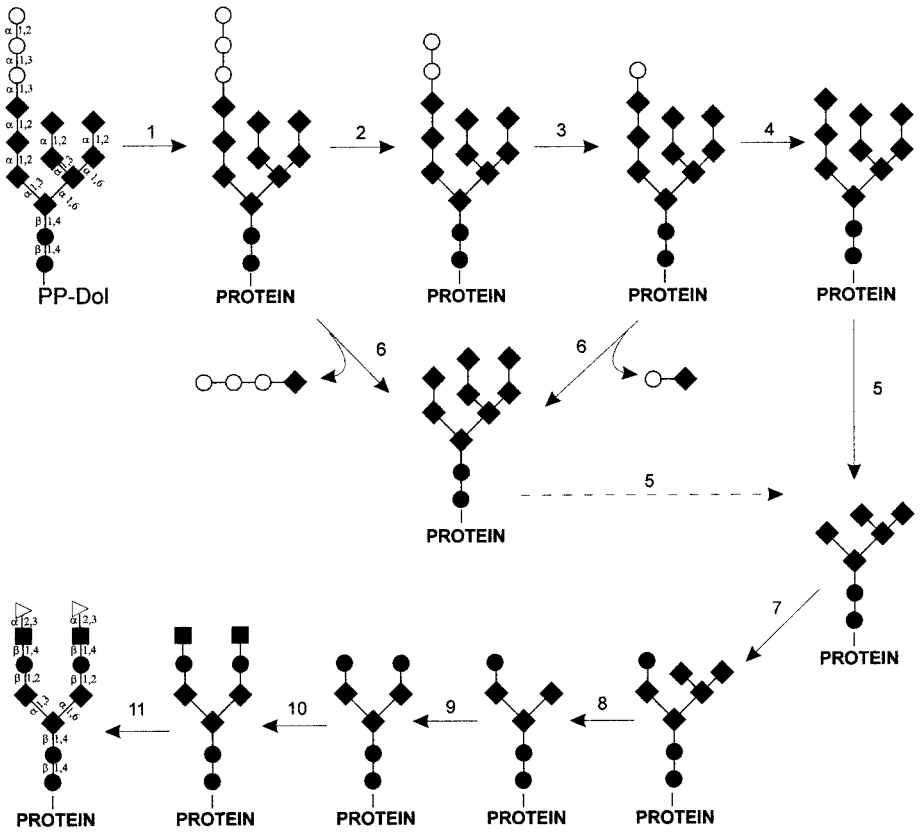

Figure 1 Biosynthetic pathway of a di-antennary N-glycan of a glycoprotein. The enzymatic steps are (1) oligosaccharyltransferase transfers the precursor oligosaccharide from dolichol pyrophosphate (PP-Dol) to the nascent protein; (2) α-glucosidase I removes distal (α1-2)-linked Glc; (3, 4) α-glucosidase II removes the (α1-3)-linked Glc residues stepwise; (5) different α-mannosidases (α-11,2-mannosidase, Man_9-mannosidase and α-mannosidase I) are responsible for the removal of the (α1-2)-linked Man residues; (6) endo-α-1,2-mannosidase removes Glc_3Man, creating the possibility of a detour along the dotted arrow; (7) *N*-acetylglucosaminyltransferase I adds the first GlcNAc residue at a specific Man residue; (8) α-mannosidase II removes the two terminal Man residues; (9) *N*-acetylglucosaminyltransferase II adds a GlcNAc residue to the newly generated terminal Man residue; (10) β-1,4-galactosyltransferase adds a Gal residue on each GlcNAc residue; (11) α-2,3-sialyltransferase terminates the glycan with a Neu5Ac residue on each Gal residue. ○ = glucose (Glc); ◆ = mannose (Man); ● = *N*-acetylglucosamine (GlcNAc); ■ = galactose (Gal); ▷ = *N*-acetylneuraminic acid (Neu5Ac).

601785, MIM 603147, MIM 602616, MIM 154550, and MIM 601110). Of the latter, several variants have been described, clinically presenting as multisystem disorders mainly caused by deficiencies of the enzymes providing sugar donor molecules for the synthesis of the precursor $Glc_3Man_9GlcNAc_2$-PP-Dol (Jaeken et al. 1994; Van Schaftingen and Jaeken 1995; de Koning et al. 1998; Korner et al. 1998, Keir et al. 1999). Genetic defects in one of the trimming enzymes in the early part of N-linked oligosaccharide processing, including glucosidase I, glucosidase II, and various specific α-1,2-mannosidases, have hitherto not been observed in humans or in other higher organisms.

Some inborn diseases related to abnormal glycoconjugate metabolism have been diagnosed by the detection of accumulating unusual carbohydrate-containing material in the patient's urine (Montreuil et al. 1996*b*). Many of these products are structurally homologous to carbohydrate sequences found in the glycans of glycoproteins. Their structures provide indirect information on errors in the biosynthesis. In this report, we describe the detection and structural analysis of an unknown oligosaccharide in the urine of a young infant. Together with morphological, enzymatic, and genetic studies, this analysis has led to the discovery of a new inborn disease with fatal outcome, resulting from a severe deficiency of glucosidase I.

Subjects and Methods

Case Report

The proband, born at 36 wk of gestation after an uneventful pregnancy and delivery, was the first child of consanguineous parents (second cousins). She had a birth weight of 2,540 g, a length of 48 cm, and a head

circumference of 33 cm. Marked generalized hypotonia and hypomotility were noticed, as were dysmorphic features, including a prominent occiput, short palpebral fissures, long eyelashes, broad nose, retrognathia, high arched palate, generalized edema, and hypoplastic genitalia. Her hands were clenched and her fingers overlapped, second over third and fifth over fourth. A band of alopecia was seen on both parietal areas of the skull. A thoracic scoliosis was present. Gastric tube feeding was necessary. Hypoventilation and frequent apneas, already present from birth, evolved to respiratory insufficiency, which required intubation and supportive ventilation at day 28. The proband had a remarkable intolerance to the administration of fluid and suffered from lung edema. Her liver became enlarged. Routine urinanalysis was normal. Urinary organic and amino acid and serum amino acid profiles were normal. Screening with thin-layer chromatography (TLC) for oligosaccharides in the urine revealed the predominant presence of one unidentified band. Activities of several lysosomal enzymes were normal in WBC (α-mannosidase, β-galactosidase, β-glucuronidase, β-hexosaminidase, α-fucosidase, sphingomyelinase). Serum immunoglobulines were normal, except for IgA, which was undetectably low. The karyotype was 46, XX. Her blood group was A rhesus positive. Seizures characterized by rhythmic clonic jerks of the left arm started at day 21 and later became more generalized, as they were associated with rhythmic vertical eye movements and tonic spasms of the limbs. A suppression-burst pattern was seen on the EEG. Brain MRI was normal. Electrodiagnostic studies showed evidence of a demyelinating polyneuropathy with motor nerve conduction velocities of 10 m/sec in the lower and 14 m/sec in the upper limbs. Muscle action potentials had low amplitudes. Visual evoked responses were flat, as was brain stem response audiometry. Liver, muscle, and nerve biopsies were performed at day 34. Septicemia caused by *Escherichia coli* occurred twice (at days 17 and 52). Despite maximal supportive therapy, the patient's general condition deteriorated. During the following weeks, her liver became increasingly enlarged, reaching 7 cm below the ribs. Aspartate aminotransferase was 80 IU/L (<58), alanine aminotransferase was 34 IU/L (<51), and activated partial thromboplastin time was 63.4 sec (<37). At age 2 mo, her body weight was 3,350 g, her length was 54 cm, and her head circumference was 36 cm. Seizures occurred more frequently and the patient lapsed gradually into a stuporous state. Artificial ventilation was stopped at day 74. Ten minutes later the patient expired. Liver and skin specimens were taken 1 h after death. The brain was removed 1 d later.

Morphological Studies

Muscle biopsy specimens were examined by means of histoenzymology and electron microscopy (De Cauwer et al. 1997). Specimens of nerve and skin samples were examined in semithin sections by light microscopy and then by electron microscopy. The pathology study of the central nervous system was done according to described techniques (Martin 1995). A liver biopsy taken at age 4 wk and a postmortem liver sample were fixed by means of 4% formaldehyde in 0.12 M sodium cacodylate buffer and were studied, as reported elsewhere (Roels et al. 1995).

Isolation and Characterization of the Urinary Oligosaccharide

Urine from the patient (300 ml) was lyophilized and the residue dissolved in 15 ml distilled water. The solution was centrifuged and the supernatant applied in 5-ml aliquots to a Bio-Gel P-2 column (68 × 1.6 cm). The column was eluted with water at a flow rate of 14 ml/h, and the eluate was monitored with a differential refractometer. Fractions were screened by TLC (Humbel and Collart 1975), and those containing the orcinol-positive oligosaccharide, corresponding with the original TLC-band, were combined. Purification was then done by high-pH anion-exchange chromatography on a Dionex LC system equipped with a CarboPac PA-1 column (250 × 4 mm), by means of a gold electrode and triple-pulse amperometry for detection. The column was eluted with a linear gradient of 25–115 mM sodium acetate in 0.1 M NaOH for 25 min at a flow rate of 4 ml/min. Monosaccharide and chemical link analysis were performed as described (Kamerling and Vliegenthart 1989; Gerwig et al. 1993). Positive-ion matrix-assisted laser desorption time-of-flight (MALDI-TOF) mass spectra were recorded with a Voyager-DE (PerSeptive Biosystems) instrument, which was equipped with a VSL-337ND-N_2 laser, operating at an accelerating voltage of 24 kV (grid voltage 92.5%, ion guide wire voltage 0.01%), and which used 2,5-dihydroxybenzoic acid as a matrix. High-resolution 500-MHz ^{1}H NMR experiments, including two-dimensional total correlation spectroscopy (TOCSY) and two-dimensional rotating frame nuclear Overhauser enhancement spectroscopy (ROESY), were performed on a Bruker AMX-500 NMR spectrometer (Bijvoet Center, Department of Nuclear Magnetic Resonance Spectroscopy) at 300 K in D_2O (Vliegenthart et al. 1983; Hård and Vliegenthart 1993).

Enzyme Assays

A skin biopsy was obtained from the patient, from both her healthy parents, and from age-matched controls. Fibroblast cell cultures were established under standard conditions. Specimens of liver were obtained 1 h after death, were immediately frozen in liquid nitrogen, and were stored at −80°C. Control postmortem liver specimens were obtained from newborn and young

children who had died of unrelated diseases. One volume of liver specimen or fibroblast cells was suspended in 9 vol of either buffer A (10 mM sodium phosphate, pH 6.8, containing 0.2% polyoxyethylene 20 cetyl ether, 50 μM phenylmethanesulphonylfluoride and 1 μg/ml leupeptine) or buffer B (50 mM sodium phosphate, pH 6.5, containing 1% Thesit, 50 μM phenylmethanesulphonylfluoride and 1 μg/ml leupeptine), and then was disrupted by means of a motor-driven glass/teflon homogenizer. The homogenates were centrifuged at 5,600 × *g* for 1 min and the supernatants assayed for glucosidase I, glucosidase II, Man_9-mannosidase and endo-α-1,2-mannosidase activity. Hydrolysis by glucosidase I and glucosidase II of fluorescent tetramethylrhodamine (TMR)-labeled trisaccharide Glc(α1-2)Glc(α1-3)Glc(α1-O)-$(CH_2)_8COOCH_3$ and TMR-labeled disaccharide Glc(α1–3)Glc(α1-O)-$(CH_2)_8COOCH_3$, respectively, was measured by incubation of 15 μl of the homogenates (containing 50–250 μg total protein) in buffer A with 5 μl of a 2-mM solution of the corresponding synthetic substrate in a total volume of 20 μl at 37°C (Scaman et al. 1996). At various time intervals, 0.5-μl samples were removed and analyzed on silica gel 60 F_{254} plates, which were developed in 2-propanol:water:NH_4OH (7:2:1 [v/v/v]). Cleavage products were quantified directly on TLC plates by means of a Biometra Biodoc II system (Westburg) and a LumiAnalyst 3.0 program (Boehringer).

For measuring glucosidase I and II activities with the radiolabeled oligosaccharide processing intermediates, 25-μl aliquots of liver or fibroblast cell homogenates prepared in buffer B (100–200 μg protein) were incubated at 37°C with 5 μl of an aqueous stock solution containing 200 cpm/μl of [^{14}C]$Glc_3Man_9GlcNAc_2$ or [^{14}C]$Glc_2Man_9GlcNAc_2$. At given times, the reaction was stopped by the addition of 30 μl acetic acid and the cleavage products subjected to paper chromatography by means of 2-propanol:acetic acid:water (29:4:9 [v/v/v]). Substrate hydrolysis was determined as described (Bause et al. 1989). The activity of Man_9-mannosidase was assayed under identical conditions with the use of 1,000 cpm of either [^{14}C]labeled $Man_9GlcNAc_2$ or $Man_5GlcNAc_2$ as the substrate (Bause et al. 1992). For the determination of endo-α-1,2-mannosidase activity, 25 μl of the homogenates were incubated with 1,000 cpm of [^{14}C]$Glc_3Man_9GlcNAc_2$ at 37°C, for 24 h and for 48 h, in the presence of 1 mM EDTA and 2 mM of the glucosidase I/II inhibitor 1-deoxynojirimycin, in order to prevent nonspecific substrate degradation (Bause and Burbach 1996). Samples were chromatographed with the more polar solvent (2-propanol:acetic acid:water; 29:8:15 [v/v/v]), to separate [^{14}C]Glc_3Man from uncleaved substrate. [^{14}C]$Glc_{3\text{-}1}Man_9GlcNAc_2$, [^{14}C]$Man_9GlcNAc_2$ and [^{14}C]$Man_5GlcNAc_2$ were synthesized as described elsewhere (Hettkamp et al. 1982; Schweden et al. 1986*b*). Radioactivity was determined with the use of Bray's solution as the counting fluid.

SDS-PAGE and Immunoblotting

Liver tissue and fibroblast cells were homogenized in buffer B and aliquots of the homogenates (50–100 μg protein) were diluted with 1 vol of 125 mM Tris/HCl, pH 6.8, containing 4% SDS and 10% 2-mercaptoethanol. The samples were subjected to SDS-PAGE, according to Laemmli (1970), followed by electrophoretic transfer onto nitrocellulose. The protein replica was incubated with rabbit polyclonal antibodies raised against glucosidase I and glucosidase II, respectively (Bause et al. 1989; Hentges and Bause 1997). Antigen-antibody complexes were detected with a goat anti-(rabbit IgG) antibody-alkaline phosphatase conjugate by staining with 5-bromo-4-chloro-3-indolyl phosphate and Nitro Blue tetrazolium chloride. Protein was determined according to the Lowry (Lowry et al. 1951) or Bramhall (Bramhall et al. 1969) procedure, with the use of bovine serum albumin as a standard.

Molecular Analysis of the Glucosidase I Gene

Total RNA was prepared from the fibroblasts by the use of Trizol™ (Life Technology), and first-strand cDNA was synthesized by M-MLV reversed transcriptase (Life Technology). Genomic DNA was extracted from peripheral blood leukocytes by the Qiagen-Blood miniprep kit (Qiagen) or from the fibroblast cultures by means of the Easy DNA kit (Invitrogen), according to the manufacturer's instructions. Oligonucleotide primers were designed on the basis of the cDNA structure of the glucosidase I gene (HSAGLUCIE, Accession NR. X87237), to obtain seven overlapping PCR fragments amplifying the total cDNA sequence. Primer sequences, conditions, and fragment lengths are given in table 1. The following numbering system was used: nt 1 is the first nt from exon 1, and the amino acid numbering starts with the first Met residue. The start codon begins at nt 132. The glucosidase I cDNA sequences from the proband and both her parents were amplified in seven overlapping fragments and were cloned with the use of the TOPO TA Cloning kit, according to the manufacturer's instructions (Invitrogen). Clones were picked, lysed with NaOH, and amplified with the use of primers flanking the insertion point in the vector. These amplimers were column purified (Concert Rapid PCR purification, Life Technology) and directly sequenced. For each fragment, $\geqslant$10 different clones were evaluated. Sequencing results were confirmed on genomic DNA. Both identified mutations were detectable on the genomic DNA by use of the same cDNA primers. For the confirmation of the R486T substitution, the primers Glu1-1395F and Glu1-1963R were used. The resulting amplimers were digested

Table 1

Oligonucleotide Primers for RT-PCR Amplification of the Complete Coding Region of the Glucosidase I Gene

Primer Pair	Primer Sequence	Annealing Temperature (°C)	Fragment Size (bp)
Glu1-3F	5′-CGCTGGCTGGCAGGTGTCGCTAA-3′		
Glu1-455R	5′-GGTTTCGGGCTGCGGGTCT-3′	60	471
Glu1-368F	5′-CTGTGTTGCCTGCCGACTCC-3′		
Glu1-880R	5′-TGCCATACTTGGGGGCTGTA-3′	60	532
Glu1-801F	5′-CAAGGGGCAGTTGAAGTTTA-3′		
Glu1-1100R	5′-TGGAATTTTCAGGGTCACCT-3′	56	319
Glu1-1051F	5′-GAGGACAGAGGTCCAAGTGG-3′		
Glu1-1433R	5′-GGAGGGCACTGCTGTAAAAA-3′	57.5	403
Glu1-1395F	5′-GCAGAAGGTGGACCCAGCCCTCTTT-3′		
Glu1-1963R	5′-TGCTCTGCCAGCCGCGTCAG-3′	62.5	588
Glu1-1900F	5′-CACCCTTCAGTAACCGAGCGGCACC-3′		
Glu1-2376R	5′-GCCACACAGCACCCCGCCAGTAG-3′	62.5	499
Glu1-2306F	5′-CCTTTGGTTTACGCTCCCTT-3′		
Glu1-2806R	5′-ATAGACTCTGGATTCACATTCACCC-3′	56.5	525
Glu1-M2066F	5′-GGGCCCCAGAGCTAGGGGTC-3′		
Glu1-2376R	As above	59	333

with endonuclease *Bsm*FI, as the base change created an additional restriction site for this enzyme. For detection of the base change F652L, a mismatch oligonucleotide primer Glu1-M2066F was developed, containing a mismatch at position −4 at the 3′ end of the primer. As such, a restriction site for the enzyme *Ava*II is created in the wild-type sequence and abolished by the base change. To distinguish the normal from the mutant restriction pattern, a double digest was performed with the endonuclease *Pst*I. Genomic DNA from 100 normal control samples was amplified and digested with the respective enzymes.

Results

Morphological Studies

Light microscopy of the liver revealed proliferation and dilatation of bile ducts enclosed by fibrotic septa (cholangiofibrosis) (fig. 2*A*). At the periphery of these fibrotic septa, numerous macrophages were seen. Parenchymal cells showed macrovesicular steatosis. Bile thrombi were seen in the parenchymal cells and in bile ducts. The lysosomes in the macrophages were enlarged. In the parenchymal cells, the lysosomes were mostly normal but numerous. Iron storage was noticed in the macrophages lining the fibrotic septa and in a few parenchymal cells. In the 6 wk between biopsy and autopsy, fibrotic septa, fat accumulation, and iron storage had clearly increased.

Electron microscopy showed that parenchymal cells contained numerous inclusions consisting of concentrically arranged lamellae (myelin-like figures) (fig. 2*B*). The lamellae were electron dense and separated from each other by an electron-lucent equidistant space. The configuration as a whole enclosed an electron-lucent inner space containing fine granular material. The lamellae at the periphery of these configurations often formed long, irregular extensions into the cytoplasm. Some were seen in close proximity to lipid droplets. Similar structures were found in bile canaliculi, bile duct lumina, and sinusoids. At these extracellular locations, the fine equidistant spacing of the lamellae was less well preserved. Lamellar configurations were also found in lysosomes of macrophages. Apart from the presence of the lamellar material and widening of the pericanalicular ectoplasm of the hepatocytes, apparent ultrastructural alterations were not noticed.

The brain weighed 492 g (normal 411 ± 55). Microscopic examination showed myelination in the corona radiata, geniculocalcarine tract at the level of the external sagittal stratum, corpus callosum, capsula interna, tracts in the tegmentum of the brain stem and at the level of the inferior olivary nuclear complex. Myelination was slightly delayed, but myelination glia was present, and morphological evidence of impaired oligodendrocyte differentiation was not found. In the upper cortical layers, small pyramidal cells were ballooned and did not stain with Sudan III or with PAS. Such ballooning was found in neurons of all parts of the cortex (fig. 3*A*); in pyramidal cells in the Sommer's field of the hippocampus; and in some neurons of the reticular formation of the brain stem, pons, and medulla, such as the nucleus dorsalis raphae or nucleus pontis centralis oralis. Similar features were found in the superior olivary nucleus, dorsal motor nucleus of the Xth cranial nerve, and in the lateral cuneate nucleus. Purkinje cells were normal, but neurons of the dentate nucleus were slightly swollen.

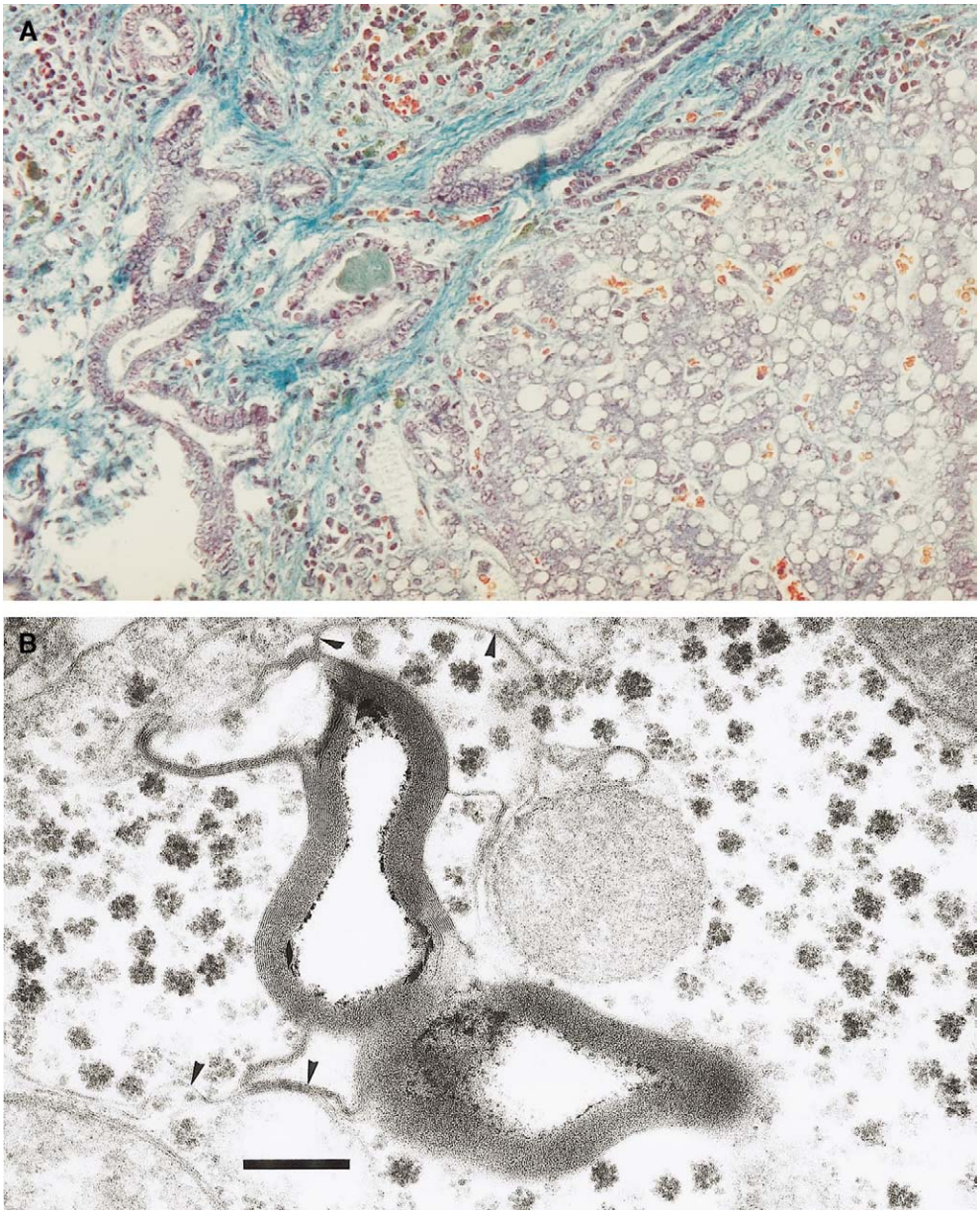

Figure 2 Morphological aspects of liver tissue from the patient. *A*, Autopsy liver cryostat section showing proliferation and dilatation of bile ducts enclosed by fibrotic septa. The parenchymal cells show a glandular rearrangement and contain numerous macroglobular lipid droplets (Trichrome stain). *B*, Electron-microscopic image of myelin-like lamellar profile in the cytoplasm of a hepatocyte. The equidistant lamellae form dense configurations that are dispersed at their periphery. M = mitochondrion. Original magnifications: A, × 250; B, × 24,000; scale bar = 0.5 μm.

Some neuronal losses were detected in the lateral parts of the inferior olivary nucleus.

Electron microscopy revealed large amounts of empty, membrane-bound vacuoles in neurons of the frontal and occipital lobes (fig. 3*B* and *C*). The vacuoles with diameters varying from 1–1.5 μm were surrounded by a single membrane and did not contain lamellar or fibrillogranular material. Dilated ergastoplasm was found in the same neurons. On one occasion, a membrane-bound vacuole containing many small bodies with lamellar profiles was found ("polymorphous cytoplasmic body"). Light- and electron-microscopic examination of skin and peripheral nerve revealed no significant abnormalities.

Isolation and Identification of the Urinary Oligosaccharide

TLC of the patient's urine (fig. 4) showed an intense carbohydrate-positive band not detected in controls.

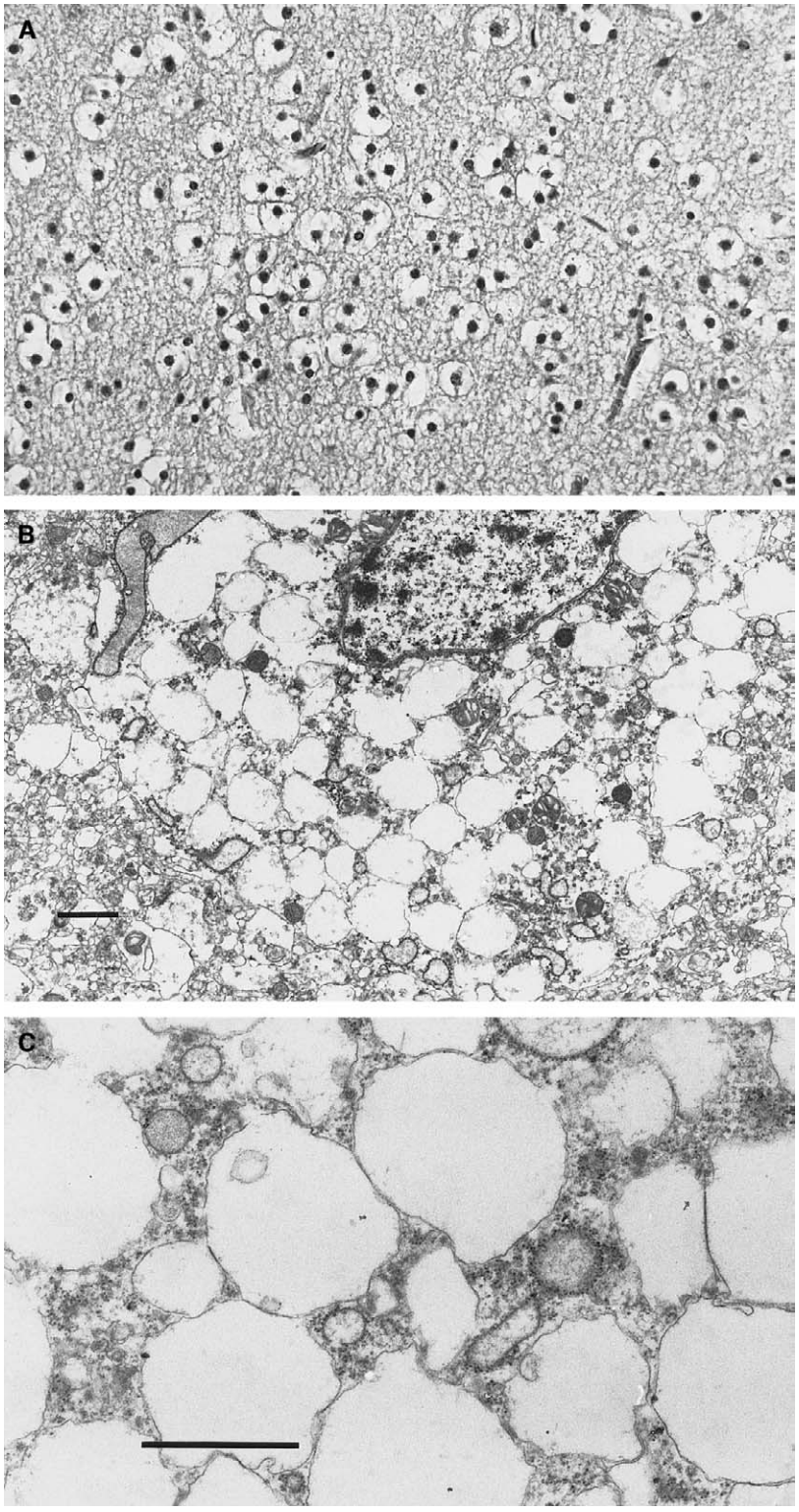

Figure 3 Morphological aspects of the brain. *A,* Light-microscopic examination of the cerebral cortex at the level of the gyrus frontalis superior: swelling of nearly all neuronal perikarya while a small area of cytoplasma around the nucleus remains preserved (formalin fixation, embedding in paraffin, HE-stain, magnification × 350). *B,* Electron micrograph of a cortical neuron: numerous membrane-bound, empty-looking vacuoles are present in the neuronal perikaryon. Dilated ergastoplasm is also found. *C,* At higher magnification, the limiting membrane of the empty-looking vacuoles is very easy to distinguish. In the center there is also a dilatation of the endoplasmic reticulum. Fixation in 4% buffered glutaraldehyde, buffered 2% osmium tetroxide postfixation, embedding in araldite, staining with uranyl acetate and lead citrate; scale bar = 1 μm.

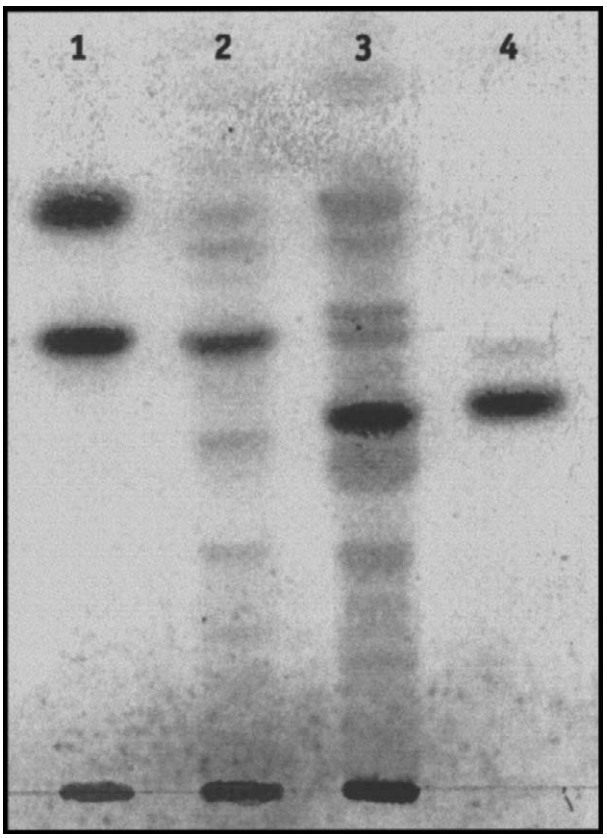

Figure 4 TLC. Lane 1, standard mixture of glucose and lactose; lane 2, control urine; lane 3, patient's urine; lane 4, isolated tetrasaccharide. TLC was performed on Kieselgel 60 F_{254} plates (0.2 mm; Merck) with the use of n-butanol:acetic acid:water (2:1:1 [v/v/v]) (Humbel and Collart 1975). Bands were visualized by spraying with a solution of orcinol/sulfuric acid and heating for 5 min at 130°C.

This compound was isolated and purified by sequential gel filtration and high-pH anion-exchange chromatography. MALDI-TOF spectrometry of the free ($[M+Na]^+$ at *m/z* 689) and permethylated ($[M+Na]^+$ at *m/z* 885) product indicated a neutral tetrasaccharide $Hexose_4$. Monosaccharide analysis of the purified compound revealed the presence of Glc and Man in a molar ratio of 3:1. After reduction with $NaBH_4$, monosaccharide analysis yielded Glc and mannitol in a molar ratio of 3:1, showing that Man occupied the reducing end. Chemical bond analysis, including gas-liquid chromatography/mass spectrometry of the partially methylated alditol acetates, demonstrated a terminal Glc, a 2- and a 3-substituted Glc and a 3-substituted Man. The sequence of the internal Glc residues and the anomeric configurations of the constituting monosaccharides were established by ^{1}H-NMR spectroscopy comprising one-dimensional (fig. 5) and two-dimensional (TOCSY and ROESY) measurements. The structure proved to be the N-glycan fragment Glc(α1-2)Glc(α1-3)Glc(α1-3)Man of glycoproteins.

Accumulation of Glc_3Man in the Urine Is Caused by Glucosidase I Deficiency

The presence of Glc(α1-2)Glc(α1-3)Glc(α1-3)Man in the urine of the patient suggested that glucosidase I, the enzyme cleaving specifically the distal α1-2-glucose from the N-linked oligosaccharide precursor, was deficient. Since $Glc_3Man_9GlcNAc_2$ is thus not processed in the endoplasmic reticulum, generation of the Glc_3Man tetrasaccharide must result from endo-α1,2-mannosidase activity in the Golgi. Homogenates from liver tissue and skin fibroblasts were not able to degrade either synthetic TMR-labeled Glc(α1-2)Glc(α1-3)Glc(α1-O)-$(CH_2)_8COOCH_3$ (fig. 6*A* and *B*), or the natural glucosidase I substrate $[^{14}C]Glc_3Man_9GlcNAc_2$ (fig. 6*C* and *D*), supporting the hypothesis that glucosidase I activity was absent. Residual glucosidase I activity measured with both substrates was <3% in either cell type. Under identical conditions, however, the activity of other processing enzymes, including Man_9-mannosidase (Fig. 6*C* and *D*), glucosidase II and endo-α-1,2-mannosidase (data not shown), was unchanged.

The molecular reason for the glucosidase I deficiency was studied further by analyzing homogenates from liver tissue and cultured skin fibroblasts by SDS-PAGE, followed by immunoblotting, with the use of polyclonal antibodies raised against glucosidase I and against the large α-subunit of the glucosidase II complex. Immunostaining of glucosidase I showed strongly decreased amounts of protein in liver homogenates from the patient compared to age-matched controls (fig. 7). The immunoreaction for glucosidase I from cultured skin fibroblasts was positive, although less intense than for controls. Similar amounts of the glucosidase II α-subunit were detected immunologically in homogenates from cells of the patient and of controls. This last observation excludes the possibility that any differences in immunostaining were due to tissue storage or workup procedures.

In cultured fibroblasts, cells from both parents' glucosidase I activity, as calculated from initial cleavage rates, were found to be ~50% of that for age-matched controls, whereas activities for Man_9-mannosidase (fig. 8) and glucosidase II (data not shown) were normal.

Molecular Analysis of the Glucosidase I Gene

The total glucosidase I cDNA sequence from the proband and both parents were amplified and sequenced. The cDNA from the proband disclosed two base changes: (1) one allele harbored a G→C transition at nt 1587, resulting in the substitution of Arg at position 486 by Thr (R486T), and (2) on the other allele a T→C transition at nt 2085 resulted in the substitution of Phe at position 652 by Leu (F652L). The proband and the mother were found to be heterozygous for the G→C transition, whereas the proband and the father were

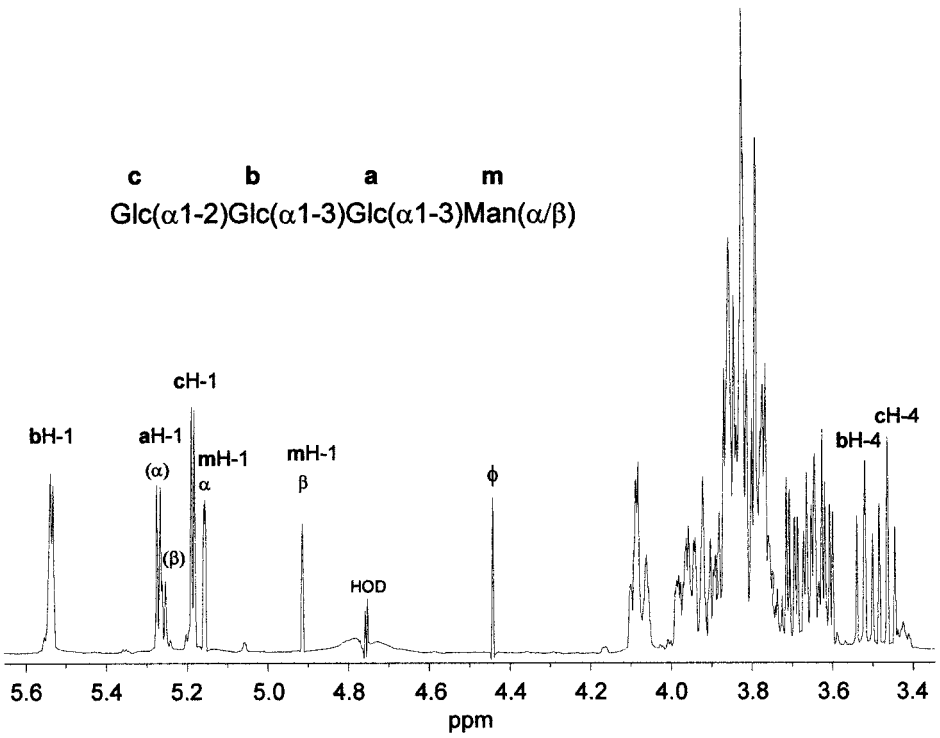

Figure 5 One-dimensional 500-MHz ^{1}H-NMR spectrum of the urinary tetrasaccharide Glc(α1-2)Glc(α1-3)Glc(α1-3)Man. The spectrum was recorded in D_2O at 300 K. Chemical shifts (δ) are expressed in ppm by reference to internal acetone (δ 2.225) (Gerwig et al. 1993). ϕ, noncarbohydrate contaminant. Full assignments of the proton chemical shifts were performed by two-dimensional homonuclear TOCSY (mixing times, 20 ms and 100 ms) and ROESY (mixing time, 250 ms) experiments. The sequence of the residues followed directly from interresidual ROE connectivities. The one-dimensional ^{1}H-NMR spectrum is similar to that of the earlier reported 400-MHz spectrum of synthetic Glc(α1-2)Glc(α1-3)Glc(α1-3)Man (Ogawa et al. 1984), whereas the ^{1}H-NMR data of the Glc residues of the tetrasaccharide were in agreement with those reported for the Glc residues in the N-glycan $Glc_3Man_9GlcNAc_2$ (Ronin et al. 1987).

found to be heterozygous for the T→C transition. Amplification of genomic DNA sequences flanking both alterations confirmed the cDNA findings in the family. These base changes were not seen in 100 control DNA samples.

Discussion

The proband presented with abnormal clinical findings in the neonatal period, including severe generalized hypotonia, dysmorphic features, hypoventilation, feeding problems, and seizures. An underlying metabolic disorder was suspected because of the relentless course of the disease and the progressive hepatomegaly. Lysosomal disorders related to N-glycan catabolism were excluded because the urinary carbohydrate excretion pattern was different from that reported in patients with lysosomal exoglycosidases deficiencies (Montreuil et al. 1996*b*). A peroxisomal disorder was also unlikely because of normal concentrations of very-long-chain fatty acids, phytanic acid, and plasmalogens in the patient's serum. The finding of a normal IEF pattern of serum sialotransferrin and of β-trace protein in CSF made the diagnosis of CDGS unlikely. In the liver, the progressive cholangiofibrosis with steatosis and cholestasis was a prominent finding (fig. 2*A*). Furthermore, the concentrically arranged multilamellar inclusions detected in the cytoplasm of parenchymal cells of the patient, not confined by a lysosomal membrane, were peculiar (fig. 2*B*). These phospholipid-like structures were also present in bile canaliculi and bile duct lumina, which suggests that the lamellar configurations represented accumulated bile components (Phillipps et al. 1993). The fact that the lamellae were also seen in the sinusoids probably reflects defective bile secretion and regurgitation. In Niemann-Pick disease, membrane-like structures can also be seen but are intralysosomal and only detected in parenchymal cells and Kupffer cells. The inclusions in patients with CDGS are strictly limited to the lysosomes of parenchymal cells. In our patient, the morphological aspect of the inclusions was different from these diseases. The abnormal intraneuronal vacuoles in the cerebral cortex were empty probably because their contents were fully water soluble (fig. 3*B*). This feature ruled out the di-

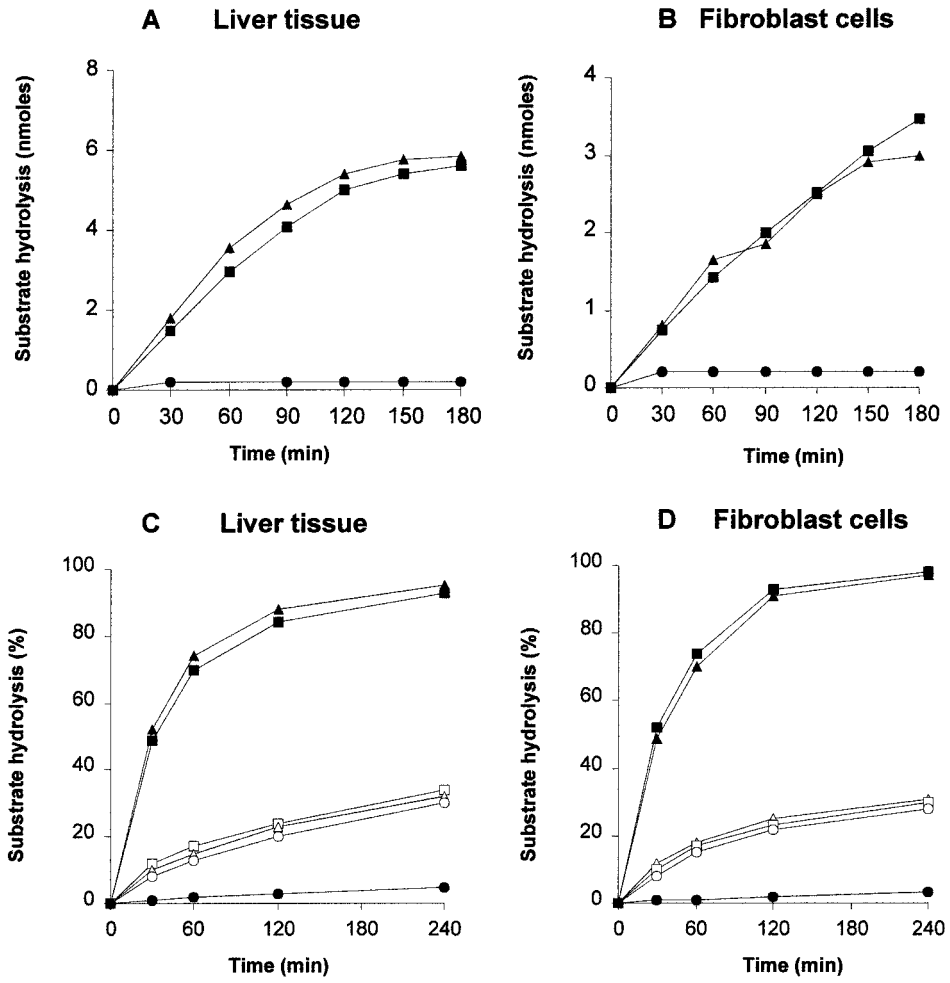

Figure 6 Glucosidase I activity is deficient in the patient. The glucosidase I activity was measured in liver tissue (*A* and *C*) and fibroblast cells (*B* and *D*) from the patient (●) and two controls (▲ and ■) by means of a fluorescently labeled (*A* and *B*) and a radioactively labeled (*C* and *D*) substrate. The activity of Man_9-mannosidase in liver tissue (*C*) and in fibroblast cells (*D*) from the patient (□) and two controls (Δ and O) is also shown.

agnosis of any sort of sphingolipidoses and has not been found by us in a whole range of lysosomal or peroxisomal diseases (Ceuterick-de Groote and Martin 1998). The neuropathological features and especially the absence of olivopontocerebellar atrophy differ from those usually described in CDGS (Eyskens et al. 1994).

The enzymatic and immunological data support the view that a severe deficiency of glucosidase I is responsible for the clinical syndrome. Thus, glucosidase I activity in cultured skin fibroblasts and liver tissue from the patient was <3% of those of control values. Fibroblasts from the mother and father, on the other hand, exhibited a phenotype expressing ~50% of glucosidase I activity compared to controls, which suggests that both parents are heterozygous for the enzyme defect. Immunoblots for liver tissue and cultured skin fibroblasts from the patient revealed decreased amounts of glucosidase I protein in both cell types, although to a different extent. One explanation for this observation could be that a catalytically inactive enzyme with normal molecular mass is synthesized by the patient but is unstable, being rapidly degraded by proteolysis. We have, however, no concrete evidence for this proposal, although increased susceptibility to proteolysis could, of course, be caused by base substitution in glucosidase I DNA, resulting in amino acid exchange and possibly defects in protein folding. This interpretation appears not unlikely because inactive glucosidase I with normal molecular mass was identified immunologically in the patient's fibroblasts. Failure to detect inactive enzyme protein in liver tissue is not necessarily inconsistent with this interpretation, since proteolysis occurs more rapidly in liver tissue than in cultured fibroblasts. Another explanation for the decreased amount of glucosidase I

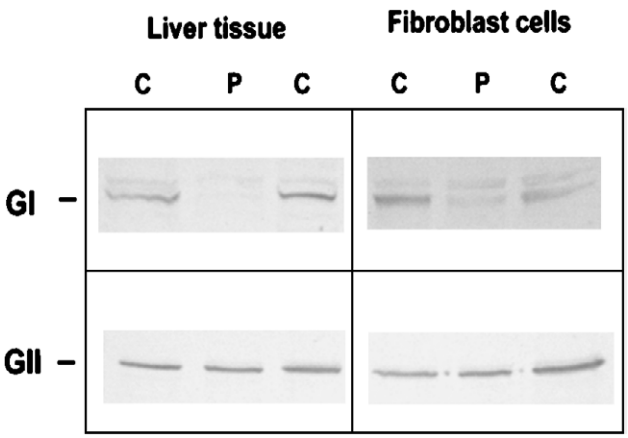

Figure 7 Immunoblots by means of polyclonal antibodies against glucosidase I (GI) and glucosidase II (GII) in liver tissue and fibroblast cells from the patient (P) and controls (C). In liver tissue from the patient, the amount of cross-reactive material (CRM) for glucosidase I is undetectably low, and that for glucosidase II is normal. In fibroblast cells, the amount of CRM for glucosidase I is significantly lower in the patient than in controls, and that for glucosidase II is normal.

protein in the patient could be a defect in glucosidase I expression, although this is unlikely given the known effects of exchanging a single base on mRNA degradation.

The excessive excretion of Glc_3Man in the patient's urine has been the initial finding that has led to the diagnosis of the glucosidase I deficiency. Removal of the distal (α1-2)-linked glucose residue from the N-linked $Glc_3Man_9GlcNAc_2$ precursor by glucosidase I is a highly specific processing step that cannot be performed by other α-glucosidases such as glucosidase II or lysosomal acid maltase. The severe glucosidase I deficiency precludes further processing steps involving glucosidase II and the various other α-mannosidases. As a consequence, the formation of complex type N-linked glycans is significantly impaired. The patient's survival for 2 mo may point to the existence of an alternate pathway already sufficiently functional to overcome, at least in part, the glucosidase I deficiency (fig. 1). Endo-α-1,2-mannosidase that is located in the Golgi cleaves N-linked $Glc_{3\text{-}1}Man_9GlcNAc_2$ oligosaccharides to yield $Glc_{3\text{-}1}Man$ units (Lubas and Spiro 1988). Glucosidase II-deficient $PHA^R2.7$ mutant mouse lymphoma cells and HepG2 cells grown in the presence of glucosidase inhibitors were found to use this endoenzyme as a bypass mechanism for N-linked oligosaccharide processing (Moore and Spiro 1990; Fujimoto and Kornfeld 1991). The glucosidase I deficiency hypothesis was supported by the observation that endo-α-D-mannosidase activity was present in cultured skin fibroblasts from the patient at comparable levels to those of controls.

Glucosidase I has been purified from various sources (Hettkamp et al. 1984; Bause et al. 1989; Schweden et al. 1986*a*; Schailubhai et al. 1987). The sequence of the full-length human glucosidase I cDNA contains 2881 bp and encodes a polypeptide of 834 amino acids corresponding to a protein with a molecular mass of ~92 kDa (Kalz-Füller et al. 1995). The gene for glucosidase I is located on chromosome 2 (p12-p13) (Kalz-Füller et al. 1996). Molecular analysis performed on cDNA isolated from fibroblast strains showed that, parental consanguinity notwithstanding, the patient was a compound heterozygote, since two base changes, resulting at position 486 in the substitution of Arg by Thr and at position 652 in the substitution of Phe by Leu, have been observed. The former mutation was found in the mother only, whereas the latter mutation was found in the father only.

In neonates with rapidly progressive neurodegenerative disease, the assay of oligosaccharides in the urine is a worthwhile test. This disorder of glycoprotein, metabolically allied to the oligosaccharidoses, represents a new entity among them but is surprisingly more rapidly progressive. Because its clinical phenotype is rather aspecific, its prevalence may be underestimated. The compound heterozygous genotype of the patient tends

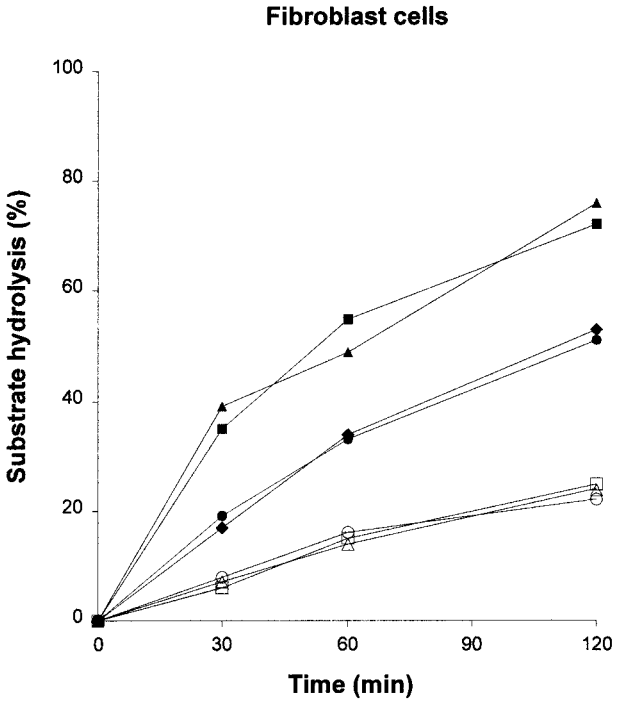

Figure 8 The initial rate of glucosidase I activity (first 30 min) in both the father and the mother is ~50% of that in controls. Glucosidase I activity was assayed with a radioactive-labeled substrate in fibroblast cells from the patient's father (●) and mother (♦) and from two controls (■ and ▲). The activities of Man_9-mannosidase in the cells from the father (□) and the mother (Δ) are comparable to those in the control (0).

to support this notion. More observations must be obtained before phenotype and pathogenesis will be better defined.

Acknowledgments

The authors wish to thank Jules Leroy, Gilles Lyon, and Chris Van Der Linden, for their critical review of the manuscript. They also thank Mrs. Edith George, for excellent technical assistance, and Chantal Ceuterick-de Groote, for the electron-microscopy work.

Electronic-Database Information

The URL for data in this article is as follows:

Online Mendelian Inheritance in Man (OMIM), http://www.ncbi.nlm.nih.gov/Omim (for mucolipidosis II [MIM 252500], mucolipidosis III [MIM 252600], leukocyte adhesion deficiency, type II [MIM 266265], congenital dyserythropoietic anemia, type II [HEMPAS disease] [MIM 224100], paroxysmal nocturnal hemoglobinuria [MIM 311770], and CDGS [MIM 601785, MIM 603147, MIM 602616, MIM 154550, and MIM 601110])

References

Bause E, Breuer W, Schweden J, Roeser R, Geyer R (1992) Effect of substrate structure on the activity of Man_9-mannosidase from pig liver involved in N-linked oligosaccharide processing. Eur J Biochem 208:451–457

Bause E, Burbach M (1996) Purification and enzymatic properties of endo-α 1,2 mannosidase from pig liver involved in oligosaccharide processing. Biol Chem 377:639–646

Bause E, Erkens R, Schweden J, Jaenicke L (1995) Purification and characterization of trimming glucosidase I from Saccharomyces cerevisiae. FEBS Lett 206:208–212

Bause E, Schweden J, Gross A, Orthen B (1989) Purification and characterization of trimming glucosidase I from pig liver. Eur J Biochem 183:661–669

Bramhall S, Noack N, Wu M, Loewenberg JR (1969) A simple colorimetric method for determination of protein. Anal Biochem 31:146–148

Ceuterick-de Groote C, Martin J-J (1998) Extracerebral biopsy in lysosomal and peroxisomal disorders: ultrastructural findings. Brain Pathol 8:121–132

De Cauwer H, Heytens L, Lubke U, Ceuterick C, Martin J-J (1997) Discordant light microscopic, electron microscopic, and in vitro contracture study findings in a family with central core disease. Clin Neuropathol 16:237–242

de Koning TJ, Dorland L, van Diggelen OP, Boonman AM, de Jong GJ, van Noort WL, De Schrijver J, et al (1998) A novel disorder of N-glycosylation due to phosphomannose isomerase deficiency. Biochem Biophys Res Commun 245: 38–42

Etzioni A, Frydman M, Pollack S, Avidor I, Phillips ML, Paulson JC, Gershoni-Baruch R (1992) Recurrent severe infections caused by a novel leukocyte adhesion deficiency. N Engl J Med 327:1789–1792

Eyskens F, Ceuterick C, Martin J-J, Janssens G, Jaeken J (1994) Carbohydrate-deficient glycoprotein syndrome with previously unreported features. Acta Paediatr 83:892–896

Fujimoto K, Kornfeld R (1991) α-Glucosidase II-deficient cells use Endo α-Mannosidase as a bypass route for N-linked oligosaccharide processing. J Biol Chem 266:3571–3578

Fukuda MN (1990) HEMPAS disease: genetic defect of glycosylation. Glycobiology 1:9–15

Gerwig GJ, Kamerling JP, Vliegenthart JF, Morag E, Lamed R, Bayer EA (1993) The nature of the carbohydrate-peptide linkage region in glycoproteins from the cellulosomes of clostridium thermocellum and bacteroides cellulosolvens. J Biol Chem 268:26956–26960

Hård K, Vliegenthart JFG (1993) Nuclear magnetic resonance spectroscopy of glycoprotein-derived carbohydrate chains. In: Fukuda M, Kobata A (eds) Glycobiology, a practical approach. Oxford University Press, Oxford, pp 223–242

Hentges A, Bause E (1997) Affinity purification and characterization of glucosidase II from pig liver. Biol Chem 378: 1031–1038

Hettkamp H, Bause E, Legler G (1982) Inhibition by nojirimycin and deoxynojirimycin of microsomal glucosidases from calf liver acting on the glycoprotein oligosaccharides $Glc_{1-3}Man_9GlcNAc_2$. Biosci Rep 2:899–906

Hettkamp H, Legler G, Bause E (1984) Purification by affinity chromatography of glucosidase I, an endoplasmic reticulum hydrolase involved in the processing of asparagine-linked oligosaccharides. Eur J Biochem 142:85–90

Humbel R, Collart M (1975) Oligosaccharides in urine of patients with glycoprotein storage disease. I. Rapid detection by thin-layer chromatography. Clin Chim Acta 60:143–145

Jaeken J, Schachter H, Carchon H, De Cock P, Coddeville B, Spik G (1994) Carbohydrate-deficient glycoprotein syndrome type II: a deficiency in Golgi-localised *N*-acetylglucosaminyltransferase II. Arch Dis Child 71:123–127

Kalz-Füller B, Bieberich E, Bause E (1995) Cloning and expression of glucosidase I from human hippocampus. Eur J Biochem 231:344–351

Kalz-Füller B, Heidrich-Kaul C, Nöthen M, Bause E, Schwanitz G (1996) Localization of the human glucosidase I gene to chromosome 2p12-p13 by fluorescence *in situ* hybridization and PCR analysis of somatic cell hybrids. Genomics 34: 442–443

Kamerling JP, Vliegenthart JFG (1989) Carbohydrates. In: Lawson AM (ed) Clinical biochemistry: principles, methods, applications. Vol 1. Walter de Gruyter, Berlin, pp 176–263

Keir G, Winchester BG, Clayton P (1999) Carbohydrate-deficient glycoprotein syndromes: inborn errors of protein glycosylation. Ann Clin Biochem 36:20–36

Korner C, Knauer R, Holzbach U, Hanefeld F, Lehle L, von Figura K (1998) Carbohydrate-deficient glycoprotein syndrome type V: deficiency of dolichyl-P-Glc:$Man_9GlcNAc_2$-PP-dolichyl glucosyltransferase. Proc Natl Acad Sci USA 95: 13200–13205

Kornfeld S (1998) Diseases of abnormal protein glycosylation: an emerging area. J Clin Invest 101:1293–1295

Laemmli UK (1970) Cleavage of structural proteins during the assembly of the head of bacteriophage T4. Nature 227: 680–685

Lowry OH, Rosebrough NJ, Farr AL, Randall RJ (1951) Protein determination by a modified Folin phenol method. J Biol Chem 193:265–275

Lubas WA, Spiro RG (1988) Evaluation of the role of rat liver golgi endo-α-D-mannosidase in processing N-linked oligosaccharides. J Biol Chem 263:3990–3998

Martin J-J (1995) Neuropathology of peroxisomal diseases. J Inher Metab Dis 18:19–33

Montreuil J, Vliegenthart JFG, Schachter H (eds) (1995) Glycoproteins: new comprehensive biochemistry. Vol 29a. Elsevier Science, Amsterdam

——— (1996*a*) Glycoproteins II. New comprehensive biochemistry. Vol 29b. Elsevier Science, Amsterdam

——— (1996*b*) Glycoproteins and diseases: new comprehensive biochemistry. Vol 30. Elsevier Science, Amsterdam

Moore SE, Spiro RG (1990) Demonstration that golgi endo-α-D-mannosidase provides a glucosidase-independent pathway for the formation of complex N-linked oligosaccharides of glycoproteins. J Biol Chem 265:13104–13112

Ogawa T, Yamamoto H, Nukada T, Kitajima T, Sugimoto M (1984) Synthetic approach to glycan chains of a glycoprotein and a proteoglycan. Pure Appl Chem 56:779–795

Philipps MJ, Lathan PS, Poucell-Hatton S (1993) Electron microscopy of human liver diseases. In: Schiff L, Schiff ER (eds) Diseases of the liver. Lippincott Company, Philadelphia, pp 189–215

Reitman ML, Varki A, Kornfeld S (1981) Fibroblasts from patients with I-cell disease and pseudo-Hurler polydystrophy are deficient in uridine 5′-diphosphate-*N*-acetylglucosamine: glycoprotein *N*-acetylglucosaminyl phosphotransferase activity. J Clin Invest 67:1574–1579

Roels F, De Prest B, De Pestel G (1995) Liver and chorion cytochemistry. J Inher Metab Dis 18 Suppl:155–171

Ronin C, Van Halbeek H, Mutsaers J, Vliegenthart JF (1987) Isolation and ^{1}H-NMR spectroscopic identification of the glucose-containing lipid-linked precursor oligosaccharide of N-linked carbohydrate chains. Glycoconj J 4:247–254

Rosse WF (1997) Paroxysmal nocturnal haemoglobinuria as a molecular disease. Medicine 76:63–93

Scaman CH, Hindsgaul O, Palcic MM, Scrivastava OP (1996) Synthesis of α-D-Glcp-(1→2)-α-D-Glcp-(1→3)-α-D-Glcp-O-$(CH_2)_8COOCH_3$ for use in the assay of α-glucosidase I activity. Carbohydr Res 296:203–213

Schailubhai K, Pratta M, Vijay I (1987) Purification and characterization of glucosidase I involved in N-linked glycoprotein processing in bovine mammary gland. Biochem J 247: 555–562

Schweden J, Borgmann C, Legler G, Bause E (1986*a*) Characterization of calf liver glucosidase I and its inhibition by basic sugar analogs. Arch Biochem Biophys 248:335–340

Schweden J, Legler G, Bause E (1986*b*) Purification and characterization of a neutral processing mannosidase from calf liver acting on $Man_9GlcNAc_2$ oligosaccharides. Eur J Biochem 157:563–570

Van Schaftingen E, Jaeken J (1995) Phosphomannomutase deficiency is a cause of carbohydrate-deficient glycoprotein syndrome. FEBS Lett 377:318–320

Vliegenthart JFG, Dorland L, Van Halbeek H (1983) High-resolution, ^{1}H-nuclear magnetic resonance spectroscopy as a tool in the structural analysis of carbohydrates related to glycoproteins. Adv Carbohydr Chem Biochem 41:209–374